

Dipole Moment and Conformation of $C_nH_{2n+1}O(CH_2CH_2O)_mH$ Investigated by the Measurements of Permittivity and FT-IR Spectra in Heptane Solutions and by Ab Initio Calculations

Mohamed El-Hefnawy, Kaori Sameshima, Toshio Matsushita, and Reiji Tanaka*

Department of Chemistry, Graduate School of Science, Osaka City University,
3-3-138 Sugimoto, Sumiyoshi-ku, Osaka 558-8585

Received November 2, 2005; E-mail: rtanaka@sci.osaka-cu.ac.jp

The apparent dipole moments (μ) of 2-methoxyethanol (C_1E_1), 2-ethoxyethanol (C_2E_1), 2-(2-methoxyethoxy)-ethanol (C_1E_2), and 2-(2-ethoxyethoxy)ethanol (C_2E_2) were determined in heptane solutions for the mole fraction range of $0 < x < 0.03$ at $T = 298.15$ K. To calculate μ values the molar volumes for these solutions and the refractive indices of the pure components were determined at $T = 298.15$ K. FT-IR spectra for these solutions were also measured at $T = 298$ K. The conformations of these compounds and that of the dimer of C_1E_1 were predicted by ab initio calculations. In order to compare the calculated results with experimental, a statistical calculation was performed. The calculated conformers of the isolated molecules correlated well with the experimental results of the dipole moment and the IR spectra.

Polyethylene glycol monoalkyl ether, $C_nH_{2n+1}O(CH_2CH_2O)_mH$ (C_nE_m), is one of the most popular emulsifiers because one can control the hydrophile–lipophile balance of the surfactant by changing the poly(oxyethylene) chain length.[1] We were interested in the aggregation process for this class of molecules in non-polar solvents by changing the amount ratio of water added to the surfactant, and found that the chain length of the hydrophilic group was a characteristic parameter as was the chain length of linear hydrocarbons used as a non-polar solvent by the measurements of heat capacity[2,3] and enthalpy of dilution.[4] We concluded that the van der Waals forces acting among the hydrophilic groups of solute dictates the aggregation of the surfactants more than the intermolecular hydrogen bonds. Therefore, studying the conformation of the oxyethylene group is important from the view point of molecular interaction in solutions. Many authors have reported the infrared and/or Raman spectra for these molecules and discussed about the intra- and intermolecular hydrogen bond.[5–19] The conformation of C_1E_1, prototypical molecules, has been studied by means of ab initio calculations and spectroscopic measurements.[12–15,20–23]

In this paper, we report the experimental dipole moments (μ) and the FT-IR spectra in heptane solutions at a temperature (T) of 298.15 K for 2-methoxyethanol (C_1E_1), 2-ethoxyethanol (C_2E_1), 2-(2-methoxyethoxy)ethanol (C_1E_2), and 2-(2-ethoxyethoxy)ethanol (C_2E_2). The molar volumes (V_m) and the refractive indices (n_D) for these molecules were also determined at $T = 298.15$ K to calculate the apparent dipole moments as a function of the mole fraction (x) of C_nE_m. We carried out the ab initio calculations for those molecules in the isolated state and of dimers. The thermal average values of the dipole moment predicted by theory agreed well with the experimental results.

Experimental

Materials. The compounds of C_nE_m for $n = 1$ or 2 and $m = 1$ or 2 were of Cica-special grade purchased from Kanto Chemical Co., Inc., and heptane was a Special-grade reagent of Wako Pure Chemical Industry Ltd. C_1E_1 and C_2E_1 were fractionally distilled by using a 100 cm high distillation column over magnesium ribbon after they were dried with 0.3 nm molecular sieves. Heptane was purified with the same distillation column. C_1E_2 and C_2E_2 were fractionally distilled in vacuum twice by using a 90 cm high spinning-band distillation column. The purities of the distilled fractions were checked by GLC analysis by using different columns from Shinwa Chemical Industries Ltd.: Thermon-1000/Chromosorb W-AW-DMCS was used for C_nE_m and Silicone DC 550/Shimalite NAW was used for heptane. The water in the purified liquids was examined by the Karl Fischer method.

Density Measurements. The densities (ρ) of mixtures of $\{xC_nE_m + (1-x)\text{heptane}\}$ and of pure heptane were measured using a vibrating tube densimeter (Anton Paar, DMA-602). The temperature in the jacket of the densimeter was controlled with a stability of ± 0.0003 K at $T = (298.15 \pm 0.01)$ K. The values of ρ were determined with an estimated standard uncertainty of $\pm 3 \times 10^{-6}$ g cm^{-3}. The excess molar volumes were calculated from the density values as a function of x by the relationship,

$$V_m^E = \{(1-x)M_1 + xM_2\}/\rho - (1-x)M_1/\rho^*_1 - xM_2/\rho^*_2, \quad (1)$$

where ρ denotes the density of the mixture, while ρ^*_1 and ρ^*_2 are the densities of heptane and C_nE_m in the pure state, respectively; M_1 and M_2 are the molar masses of heptane and C_nE_m, respectively. The mixtures were prepared with specially designed vessels of a volume of 10 cm^3 that avoided a change in x due to evaporation into the vapor phase above the liquid. The uncertainty in molar volume, δV_m, was propagated from the uncertainty in the mole fraction (δx) and that in the density of the mixture ($\delta\rho$). The uncertainty in x was less than 1×10^{-5}. The combined standard uncertainty in V_m was estimated to be about 1.3×10^{-3} cm^3 mol^{-1}.

Published on the web June 6, 2006; doi:10.1246/bcsj.79.845

The preparation of mixtures and the determination of density have been described previously.[24]

Refractive Index Measurements. The refractive indices for the sodium-D line (n_D) of the pure compounds were measured with an Abbe refractometer (NAR-3T, Atago Co., Ltd., Japan) at $T = (298.15 \pm 0.01)$ K with an uncertainty of ± 0.00005. The value of n_D for water was determined to compare with a literature value.

Permittivity and Dipole Moment Measurements. Measurements of the electrical capacitance (C) were carried out with an LCR meter (Hewlett-Packard, model HP-4284A) at a frequency of 30 kHz and $T = 298.15$ K. A stepwise dilution method[25–27] was applied to measure the permittivity. The electrode cell consisted of two cylindrical nickel plates. The inner cylinder had a 6 cm height and a diameter of 32 mm, and the outer one was fixed with 3 mm of clearance between the two plates. The capacitance of the cell in vacuum was about 28 pF with a lead-capacitance of 4 pF. It was immersed in an oil bath, and its temperature was controlled within ± 0.002 K. The value of C was measured with a repeatability of ± 0.0001 pF, which corresponded to an uncertainty of $\pm 3.5 \times 10^{-6}$ in the relative permittivity (ε_r).

The Fröhlich equation,[28]

$$V_m(\varepsilon_r - 1)/3\varepsilon_r = (1 - x)V^*_1(\varepsilon^*_{r,1} - 1)/(\varepsilon^*_{r,1} + 2\varepsilon_r) + xV^*_2(\varepsilon_{r,2}' - 1)/(\varepsilon_{r,2}' + 2\varepsilon_r) + 4\pi N_A x g \mu_0^2(\varepsilon_{r,2}' + 2)^2(2\varepsilon_r + 1)/27kT(\varepsilon_{r,2}' + 2\varepsilon_r)^2, \quad (2)$$

was used to calculate μ values. It is expressed in terms of the relative permittivity for the solution (ε_r), for heptane ($\varepsilon^*_{r,1}$), the molar volume of the solution (V_m), the molar volume of heptane (V^*_1), the molar volume of C_nE_m (V^*_2), and the "internal permittivity" of C_nE_m ($\varepsilon_{r,2}'$) activated by infrared radiation. Here, N_A is the Avogadro constant, k is the Boltzmann constant, and g is the "Kirkwood g-factor."[29] The Fröhlich equation is based on the cavity field and the reaction field proposed by Onsager.[30] The apparent dipole moment, μ, is defined as $\mu = (g\mu_0^2)^{1/2}$, where μ_0 denotes the dipole moment of an isolated molecule. We calculated $\varepsilon_{r,2}'$ from the Clausius–Mossotti equation, adopting the atomic polarization (P_A) that was evaluated by using the assumed relation,

$$P_E + P_A = 1.10P_E, \quad (3)$$

where P_E was calculated by the Lorenz–Lorentz equation using n_D. The limiting value of μ_0 was determined by extrapolating μ values to infinite dilution by the least-squares method. The uncertainty in μ for $x < 0.01$ increased exponentially as x decreased. The expanded uncertainty in μ_0 (with a coverage factor = 2) was estimated to be ± 0.003 D, where $1\text{ D} = 3.33564 \times 10^{-30}$ C m. The difference in the μ_0 values calculated with the Fröhlich equation and the Debye equation, commonly used for vapor phase, has been described previously.[31,32]

FT-IR Spectra Measurements. FT-IR absorption spectra were measured with a model FT/IR-7000 spectrometer (JASCO Co., Japan) at room temperature ($\approx$298 K) using a cell of a fixed path length of 0.5 mm attached with KBr windows. Each sample was recorded with 10 scans at a resolution of 2 cm^{-1}.

Method of Ab Initio Calculations. Ab initio calculations for C_nE_m and the dimer of C_1E_1 were performed by the B3LYP method.[33] The geometries of conformers of these molecules were optimized by using a 6-311+G(2d,p) basis set.[34] To improve relative energies and dipole moments, single point calculations were undertaken with 6-311+G(3d,2p) and 6-311++G(3df,3pd) basis sets.[34] For C_1E_1, 6-311++G(3df,3pd) basis sets were also used at the geometry optimization. Also, the G2 calculation[35] was performed in order to attest the reliability of the B3LYP results. Energies and vibrational frequencies of C_1E_1 dimers were also obtained with 6-311+G(3d,2p) and 6-311+G(2d,p) basis sets. All the calculations were carried out using the Gaussian 98 program system.[36]

For the molecules studied here, there exist many conformers. Their energies are close to each other and the dipole moments vary from one conformer to another. To compare the calculated dipole moments with the observed, we assumed the Boltzmann distribution for the optimized conformers.

Results and Discussion

Excess Volume and Apparent Dipole Moment. The experimental results for the purity, ρ, V_m, and n_D of the pure compounds are listed in Table 1 along with the literature values. The values of ρ and V_m^E are summarized in Table 2. A smoothing function,

$$V_m^E/(\text{cm}^3\text{ mol}^{-1}) = x(1 - x)\sum c_j x^{(j-1)}, \quad (4)$$

was fitted to the excess volumes by the least-squares method. The coefficients of c_j are listed in Table 3 with the estimated standard uncertainty (u). The capacitance for each system was measured twice to confirm the reproducibility. The μ values of two separate runs for $x < 0.003$, a relevant range to determine the μ_0 values, agreed excellently within an estimated uncertainty of ± 0.003 D. The experimental values of ε_r and μ are summarized in Table 4. In Fig. 1 (a and b), the calculated apparent dipole moments of C_nE_m observed in heptane for a mole fraction range of $0 < x < 0.03$ are represented graphically. The limiting dipole moments (μ_0) are listed in Table 5 with the literature values.

The value of μ_0 for C_1E_1 and C_2E_1 increased by replacing the polar moiety with $-O(C_2H_4O)_2H$ (compare Figs. 1a and 1b). By replacing CH_3 in C_nE_1 with C_2H_5, the value of μ_0 in-

Table 1. Densities (ρ), Molar Volumes (V_m), and Refractive Indices (n_D) at $T = 298.15$ K and Purities for Liquids

Liquid	Purity/%[a)]	$x(H_2O)$ $\times 10^{4}$[b)]	ρ(obs) /g cm^{-3}	ρ(lit) /g cm^{-3}	ρ(lit) /g cm^{-3}	V_m /cm^3 mol^{-1}	n_D (obs.)	n_D (lit.)[c)]	n_D (lit.)
Water							1.33250	1.3325029	
Heptane	99.95	1.6	0.679570	0.67957[d)]	0.67955[f)]	147.4507	1.38510	1.38511	1.38512[j)]
2-Methoxyethanol (C_1E_1)	99.99	11.0	0.960080	0.96004[e)]	0.96002[g)]	79.2584	1.40020	1.4002	1.40046[k)]
2-Ethoxyethanol (C_2E_1)	99.92	20.0	0.925042	0.92505[e)]	0.92502[g)]	97.4237	1.40585	1.4057	1.40593[f)]
2-(2-Methoxyethoxy)ethanol (C_1E_2)	99.97	10.0	1.015418	1.01591[e)]	1.0154[h)]	118.3227	1.42410	1.4245	1.4246[l)]
2-(2-Ethoxyethoxy)ethanol (C_2E_2)	99.97	37.0	0.983082	0.9841[c)]	0.9839[i)]	136.4826	1.42520	1.4254	1.4275[l)]

a) Determined with GLC analysis. b) Determined by Karl Fisher method. c) Ref. 42. d) Ref. 43. e) Ref. 44. f) Ref. 45. g) Ref. 46. h) Ref. 47. i) Ref. 48. j) Ref. 49. k) Ref. 50. l) Ref. 51.

Table 2. Densities (ρ) and Excess Molar Volumes (V_m^E) of $\{xC_nH_{2n+1}O(CH_2CH_2O)_mH, (C_nE_m) + (1-x)C_7H_{16}\}$ at $T = 298.15$ K

x	ρ /g cm^{-3}	V_m^E /cm^3 mol^{-1}	x	ρ /g cm^{-3}	V_m^E /cm^3 mol^{-1}	x	ρ /g cm^{-3}	V_m^E /cm^3 mol^{-1}	x	ρ /g cm^{-3}	V_m^E /cm^3 mol^{-1}
$xC_1E_1 + (1-x)C_7H_{16}$			$xC_2E_1 + (1-x)C_7H_{16}$			$xC_1E_2 + (1-x)C_7H_{16}$			$xC_2E_2 + (1-x)C_7H_{16}$		
0.00496	0.680100	0.048	0.00538	0.680218	0.049	0.00489	0.680699	0.039	0.00473	0.680719	0.038
0.00508	0.680114	0.049	0.00592	0.680286	0.054	0.00515	0.680760	0.042	0.00822	0.681592	0.062
0.00877	0.680534	0.079	0.00958	0.680752	0.082	0.00547	0.680832	0.044	0.01159	0.682451	0.081
0.01210	0.680923	0.104	0.01430	0.681373	0.114	0.00563	0.680873	0.045	0.01610	0.683610	0.104
0.01687	0.681502	0.136	0.01702	0.681744	0.130	0.00799	0.681428	0.063	0.01939	0.684462	0.120
0.01884	0.681752	0.147	0.02193	0.682422	0.157	0.00874	0.681608	0.067	0.02203	0.685150	0.132
0.02491	0.682506	0.185	0.02579	0.682967	0.176	0.01355	0.682786	0.094	0.02779	0.686670	0.154
0.02954	0.683104	0.210	0.03094	0.683702	0.201	0.01565	0.683306	0.105	0.03146	0.687638	0.168
0.03067	0.683257	0.214				0.02048	0.684516	0.126			
0.03843	0.684286	0.251				0.02108	0.684656	0.131			
						0.02558	0.685794	0.149			
						0.03098	0.687168	0.170			

Table 3. Coefficients (c_j) and Estimated Standard Uncertainty (u) Determined by Eq. 4 for $\{xC_nH_{2n+1}O(CH_2CH_2O)_mH, (C_nE_m) + (1-x)C_7H_{16}\}$ at $T = 298.15$ K

c_j	C_1E_1	C_2E_1	C_1E_2	C_2E_2
c_1	10.43	9.986	8.92	8.83
c_2	−158.5	−158.7	−157.6	−172
c_3	1703	1693	1663	2146
u/cm^3 mol^{-1}	1.6×10^{-3}	1.5×10^{-4}	9.0×10^{-4}	7.8×10^{-4}

creased markedly, while the effect of the same replacement for C_nE_2 was relatively small (compare the gaps between the two curves in Figs. 1a and 1b). The value of μ for C_1E_1 was constant in the region of $0 < x < 0.003$ and then decreased with increasing x. Such a feature is commonly observed for alkanols solved in non-polar solvents.[25,27,31,32,37] It is interpreted that the solutes undergo few molecular interactions in the dilute region; thereby, the μ value was kept constant. The constant range is much smaller in C_2E_1 than in C_1E_1. The values of μ for C_1E_1 and C_2E_1 decreased with increasing x due to intermolecular interactions, whereas the values of μ for C_1E_2 and C_2E_2 increased monotonously with increasing x in the region of $0 < x < 0.005$. These results suggest that the aggregation of solutes takes place even in an extremely dilute region.

FT-IR Spectra. Figure 2 shows FT-IR absorption spectra of C_1E_1 in heptane solutions for $0.001 < x < 0.013$ measured from 3300 to 3700 cm^{-1} at $T = 298$ K. A sharp peak appeared at 3610 cm^{-1} accompanied by a broad band around 3505 cm^{-1} due to the stretching vibration of the hydrogen bond. Very similar peaks were observed for C_2E_1, viz. 3610 and 3503 cm^{-1}, respectively. In both cases, the peak at 3610 cm^{-1} increased with increasing x, whereas no absorption around 3500 cm^{-1} was observed for $x < 0.002$. The absorption of the peaks around 3600 and 3500 cm^{-1} for C_1E_1 and C_2E_1 systems are plotted as a function of x in Fig. 3. The present results suggest that C_1E_1 and C_2E_1 exist in an isolated state at the very dilute region of $x < 0.002$. Therefore, the absorption around 3500 cm^{-1} is attributed to the intermolecular hydrogen bond. This conclusion is consistent with the observation of μ. Nakamura et al.[8] reported the IR spectra for polyethylene glycol monododecyl ether ($C_{12}E_m$, for $m = 1$ to 5) in CCl_4 solutions of $x = 1 \times 10^{-5}$. They found two sharp peaks at 3637 and 3605 cm^{-1} accompanied by a broad one around 3500 cm^{-1}, except for $C_{12}E_1$. Since only $C_{12}E_1$ had no absorption at 3500 cm^{-1}, they concluded that the absorption around 3500 cm^{-1} was due to the intramolecular hydrogen bond. They assigned the sharp peak at 3637 cm^{-1} to the free OH-stretching of $C_{12}E_m$. However, we found no absorption band around 3637 cm^{-1}. This peak reported by them was probably due to water contaminating the sample liquids. Prabhumirashi et al. assigned the peaks

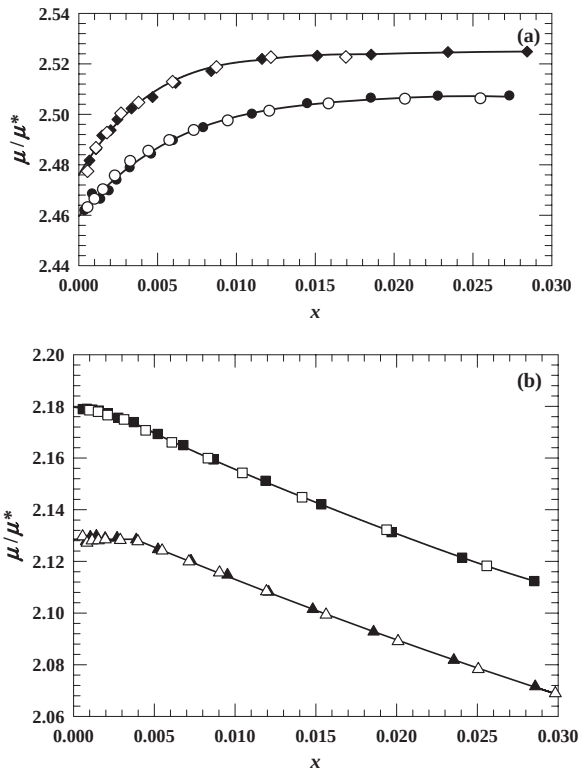

Fig. 1. Apparent dipole moments (μ) of C_nE_m vs mole fraction (x) of C_nE_m determined in heptane solutions at $T = 298.15$ K. (a): Plots for C_1E_2 and C_2E_2. C_1E_2: ◆, run 1; ◇, run 2. C_2E_2: ●, run 1; ○, run 2. (b): Plots for C_1E_1 and C_2E_1. C_1E_1: ▲, run 1; △, run 2. C_2E_1: ■, run 1; □, run 2.

Table 4. Relative Permittivities (ε_r) for $\{xC_nH_{2n+1}O(CH_2CH_2O)_mH$, $(C_nE_m) + (1-x)C_7H_{16}\}$ and Apparent Dipole Moments (μ) of C_nE_m at $T = 298.15$ K; where $\mu^* = 3.33564 \times 10^{-30}$ C m

x	ε_r	μ/μ^*	x	ε_r	μ/μ^*	x	ε_r	μ/μ^*	x	ε_r	μ/μ^*
$xC_1E_1 + (1-x)C_7H_{16}$			$xC_2E_1 + (1-x)C_7H_{16}$			$xC_1E_2 + (1-x)C_7H_{16}$			$xC_2E_2 + (1-x)C_7H_{16}$		
	run 1			run 1			run 1			run 1	
0.000561	1.916563	2.130	0.000983	1.918150	2.179	0.000555	1.917321	2.477	0.000552	1.917381	2.463
0.000835	1.917469	2.127	0.001520	1.920042	2.178	0.001089	1.919845	2.487	0.000994	1.919445	2.466
0.001145	1.918497	2.128	0.002111	1.922116	2.177	0.001786	1.923162	2.493	0.001533	1.921979	2.470
0.001535	1.919796	2.128	0.003128	1.925693	2.175	0.002678	1.927459	2.500	0.002285	1.925546	2.476
0.001965	1.921228	2.128	0.004462	1.930351	2.171	0.003792	1.932844	2.505	0.003261	1.930215	2.482
0.002892	1.924317	2.128	0.006084	1.935999	2.166	0.005950	1.943410	2.513	0.004409	1.935729	2.486
0.003980	1.927947	2.128	0.008316	1.943733	2.160	0.008728	1.957145	2.519	0.005743	1.942188	2.490
0.005482	1.932921	2.124	0.010452	1.951101	2.154	0.012185	1.974391	2.523	0.007289	1.949732	2.494
0.007143	1.938404	2.120	0.014151	1.963787	2.145	0.01694	1.998173	2.523	0.009446	1.960315	2.498
0.009036	1.944642	2.116	0.01938	1.981570	2.132				0.012076	1.973335	2.501
0.011945	1.954158	2.108	0.02558	2.002428	2.118				0.01584	1.992069	2.504
0.015630	1.966142	2.099							0.02068	2.016406	2.506
0.020085	1.980538	2.089							0.02547	2.040616	2.506
0.02505	1.996478	2.078							0.03013	2.064338	2.506
0.02983	2.011737	2.069									
	run 2			run 2			run 2			run 2	
0.000556	1.917379	2.124	0.000572	1.917491	2.179	0.000679	1.918016	2.482	0.000838	1.918761	2.469
0.000771	1.918098	2.128	0.000826	1.918386	2.179	0.001087	1.919944	2.486	0.001361	1.921193	2.467
0.001041	1.918997	2.129	0.001163	1.919573	2.179	0.001486	1.921846	2.492	0.001895	1.923707	2.470
0.001416	1.920247	2.130	0.001568	1.920999	2.178	0.002024	1.924405	2.494	0.002389	1.926058	2.474
0.001958	1.922048	2.129	0.002105	1.922888	2.177	0.002450	1.926462	2.498	0.003227	1.930057	2.479
0.014808	1.964329	2.101	0.015338	1.968641	2.142	0.018541	2.006440	2.524	0.02277	2.027080	2.507
0.018575	1.976530	2.093	0.019688	1.983391	2.131	0.02342	2.031331	2.525	0.02730	2.050087	2.507
0.02354	1.992516	2.082	0.02405	1.998099	2.121	0.02844	2.057191	2.525			
0.02858	2.008643	2.072	0.02852	2.013116	2.112						

Table 5. Limiting Dipole Moment (μ_0) of $C_nH_{2n+1}O$-$(CH_2CH_2O)_mH$, (C_nE_m) in Heptane Solution at $T = 298.15$ K; where $\mu^* = 3.33564 \times 10^{-30}$ C m

$C_nH_{2n+1}O(CH_2CH_2O)_mH$, (C_nE_m)	μ_0/μ^*	
	obs.	lit.[a)]
2-Methoxyethanol (C_1E_1)	2.129	2.04
2-Ethoxyethanol (C_2E_1)	2.180	2.08
2-(2-Methoxyethoxy)ethanol (C_1E_2)	2.476	1.6
2-(2-Ethoxyethoxy)ethanol (C_2E_2)	2.460	1.6

a) Ref. 42.

around 3475 cm^{-1} found for C_nE_1 in CCl_4 solutions to the intermolecular hydrogen bond.[9] In later reports, however, they assigned the peak found for C_nE_2[10] and C_1E_4[11] to the intramolecular hydrogen bond. Although the assignment of the IR spectra for the isolated C_nE_m was not distinct enough, ab initio calculations performed for C_1E_1 clearly demonstrated that the absorptions observed around 3640 and 3608 cm^{-1} are due to the stretching vibration of the conformer with "free" OH and that associated with the intramolecular hydrogen bond, respectively.[12,20]

Figure 4 shows the FT-IR absorption spectra of C_1E_2 in heptane solutions at 298 K. Two main peaks appeared at 3612 and 3502 cm^{-1} as in the cases of C_1E_1 and C_2E_1. Identical absorptions were observed for C_2E_2, viz. at 3611 and 3487 cm^{-1}. In both solutions, the peak around 3500 cm^{-1} increased with increasing x at the expense of the intensity around 3600 cm^{-1}. The change in the magnitude of the absorption for these peaks is plotted against x in Fig. 5. The absorption around 3500 cm^{-1}

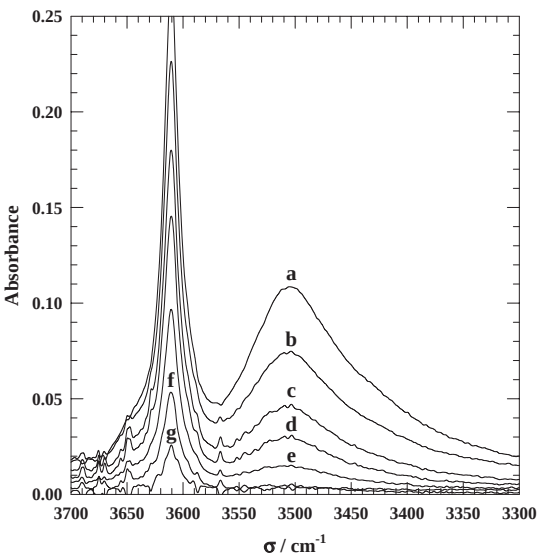

Fig. 2. FT-IR absorption spectra of C_1E_1 in heptane solutions at $T = 298$ K for various mole fractions (x): a, $x = 0.0130$; b, $x = 0.0100$; c, $x = 0.0076$; d, $x = 0.0060$; e, $x = 0.0039$; f, $x = 0.0021$; g, $x = 0.0010$.

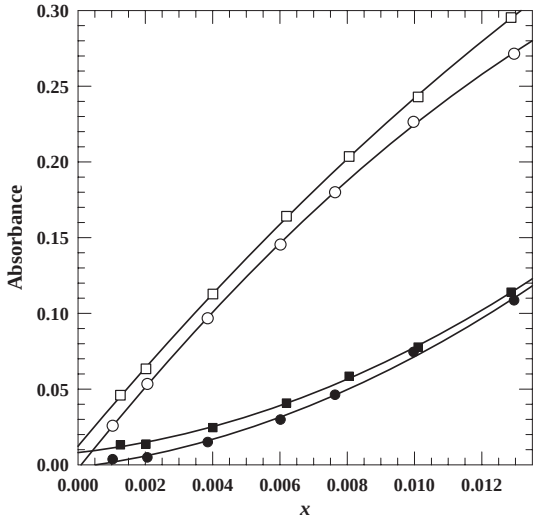

Fig. 3. Plots of absorbance change of FT-IR spectra with mole fraction (x) for C_1E_1 and C_2E_1 in heptane solutions at $T = 298$ K. C_1E_1: ○, $\sigma = 3610\,cm^{-1}$; ●, $\sigma = 3505\,cm^{-1}$. C_2E_1: □, $\sigma = 3610\,cm^{-1}$; ■, $\sigma = 3503\,cm^{-1}$. Curves are the least-squares representation.

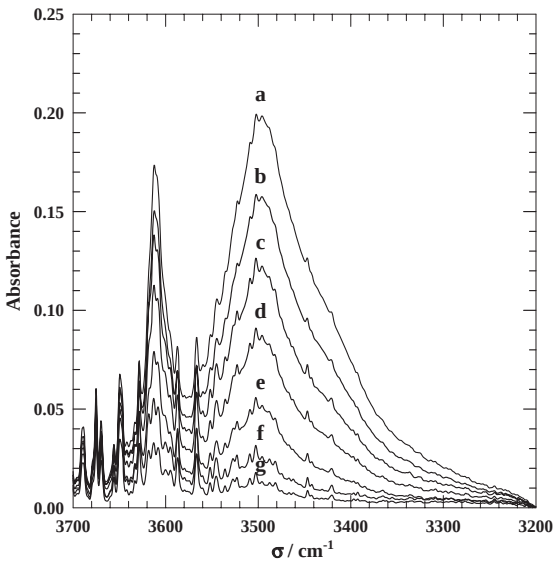

Fig. 4. FT-IR absorption spectra of C_1E_2 in heptane solutions at $T = 298$ K for various mole fractions (x): a, $x = 0.0123$; b, $x = 0.0101$; c, $x = 0.0082$; d, $x = 0.0064$; e, $x = 0.0040$; f, $x = 0.00201$; g, $x = 0.0010$. The minor peaks appearing around $3600\,cm^{-1}$ are probably due to the vapor of water.

still exists for the dilute region of $x < 0.002$. This result leads to the conclusion that C_1E_2 and C_2E_2 form intermolecular aggregates at a very dilute region because of the enhanced van der Waals force due to the longer oxyethylene group. This fact is consistent with the observation that the monotonous increment in μ occurred already from a very dilute region for these compounds. In our previous study of heat capacity measurements, we found that the aggregation of $C_{10}E_m$ for $m =$ 1–8 in alkane solutions proceeds moderately compared with that of decanol.[2,3] The measurements of the apparent molar

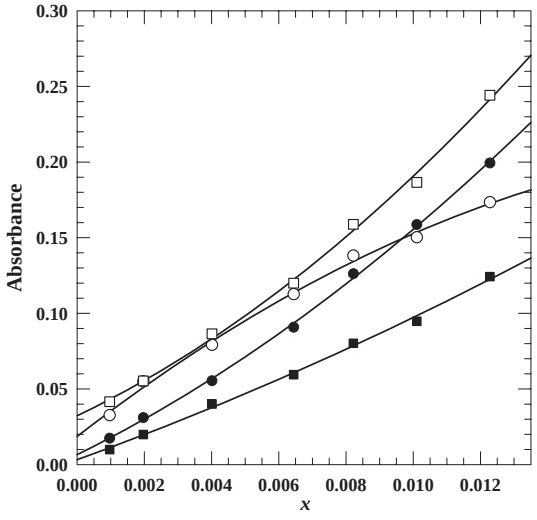

Fig. 5. Plots of absorbance changes of FT-IR spectra with mole fraction (x) for C_1E_2 and C_2E_2 in heptane solutions at $T = 298$ K. C_1E_2: ○, $\sigma = 3612\,cm^{-1}$; ●, $\sigma = 3502\,cm^{-1}$. C_2E_2: □, $\sigma = 3611\,cm^{-1}$; ■, $\sigma = 3487\,cm^{-1}$. Curves are the least-squares representation.

enthalpies of $C_{10}E_m$ diluted in alkane also showed that the aggregation occurs gradually with increasing molality of solutes.[4] The present experimental results agree with our previous conclusion obtained from these calorimetries that the van der Waals forces acting among the hydrophilic groups of solute drives the aggregation of the $C_{10}E_m$ rather than the intermolecular hydrogen bond.

Brinkley and Gupta[16] carried out careful measurements of FT-IR spectra for C_1E_1 and C_4E_1 in hexane solutions at $T =$ 308 and 318 K. They analyzed the fractions of intra- and intermolecular hydrogen bonds for the whole range of x and found that the fraction of the intra- and intermolecular hydrogen bond changed with increasing x: the fraction of intramolecular hydrogen bond dominated over the intermolecular at an extremely low x, whereas the order of the fraction was reversed at the expense of the intramolecular hydrogen bond for $x > 0.1$. They concluded that C_4E_1 possesses a more non-polar character than the corresponding alcohols. Their conclusion supports our results deduced from calorimetries.[2–4] Singelenberg et al.[19] measured IR spectra of C_nE_m in CCl_4 at a dilute concentration ($<0.001\,mol\,dm^{-3}$) to avoid intermolecular interactions. They found broad bands from 3474 to $3482\,cm^{-1}$ for C_nE_m with $m \geq$ 2 and an extra peak at $\approx 3520\,cm^{-1}$ for C_1E_m with $m \geq 3$. These absorptions were assigned to intramolecular hydrogen bonding based on a measurement at a single concentration. Since our measurements of μ indicate that the intermolecular aggregates of C_1E_2 and C_2E_2 even exist at very dilute solutions, further examination is required to characterize the bands at $\approx 3500\,cm^{-1}$ found for C_nE_m with $m \geq 3$.

Calculated Dipole Moments of C_1E_1 and C_2E_1. The conformation of C_nE_m can be characterized by the dihedral angles to describe the rotations about the single skeletal bonds of these molecules. For C_1E_1 the conformations can be classified by using three numbers.[21] The first number stands for the rotational angle of the alcohol O_1–C_1 (dihedral angle of $H_1O_1C_1C_2$), and the second and third stand for the rotational

angles of C_1–C_2 (dihedral angles of $O_1C_1C_2O_2$) and C_2–O_2 (dihedral angle of $C_1C_2O_2C_3$), respectively. The numbering of the atoms is shown in Fig. 6a. The figure 0 is assigned to the *trans* conformation, i.e., the calculated dihedral angle is near 180°. The figures 1 and 2 are used for *gauche* conformations with positive or negative dihedral angles of ±60.0°, respectively. We obtained twelve conformations for C_1E_1, as found in previous theoretical works.[21,23] The results are contained in Table 6 together with the labels such as 120 to characterize the conformers.

First, it is seen that the relative energies of the conformers are reasonably consistent through all the B3LYP calculations. The maximum discrepancies arose at B3LYP/6-311+G(2d,p)//B3LYP/6-311+G(2d,p) in comparison with the 6-311++G(3df,3pd) results. However, they are within about 1 kJ mol^{-1} and satisfying for the evaluation of the Boltzmann distribution. Larger basis sets improved the relative energies and gave very close energies. Especially, geometries obtained by 6-311+G(2d,p) basis sets reproduced well those by 6-311++(3df,3pd) basis sets, as shown in Fig. 6a and judging from the energy differences between them. The most two stable structures were 120 and 122. The energy difference was about 7 kJ mol^{-1} in favor of 120 at the B3LYP results, which was in good accord with the early MP2/6-31+G(d) calculation.[23] Then, conformers 000 and 100 of almost the same energies followed the above two. The stability of the conformers 120 and 122 may be attributed to an intramolecular hydrogen bond formed between the hydroxy hydrogen and the ethereal O atom. The distance between the H and O was 0.24 nm, as shown in Fig. 6a, which is longer than a typical hydrogen-bond distance, viz., 0.18–0.19 nm. We found that the difference of OH frequency between 000 and 120 was 40–50 cm^{-1} at the B3LYP calculations. It was much smaller than the fre-

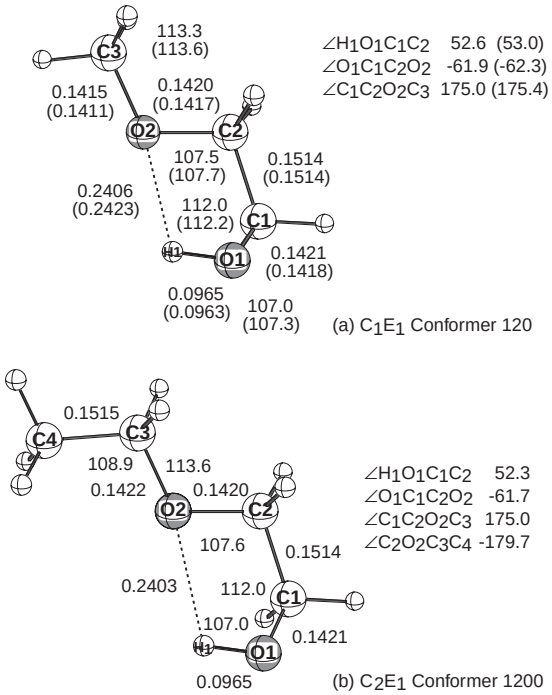

Fig. 6. Calculated geometries of C_1E_1 and C_2E_1 by the B3LYP/6-311+G(2d,p) and B3LYP/6-311++G(3df,3pd) methods in parenthesis. Units are shown in nm and degree.

Table 6. Calculated Relative Energies ΔE, Dipole Moments μ, and Thermally Averaged Dipole Moments of $CH_3OC_2H_4OH$ (C_1E_1); $\mu^* = 3.33564 \times 10^{-30}$ C m: Populations[c] of Conformers are in Parentheses

	B3LYP								G2	
	6-311+G(2d,p)//6-311+G(2d,p)		6-311+G(3d,2p)//6-311+G(2d,p)		6-311++G(3df,3pd)//6-311+G(2d,p)		6-311++G(3df,3pd)//6-311++G(3df,3pd)			
Conformation[a]	ΔE[b] /kJ mol^{-1}	μ/μ^*	ΔE[b] /kJ mol^{-1}	μ/μ^*	ΔE[b] /kJ mol^{-1}	μ/μ^*	ΔE[b] /kJ mol^{-1}	μ/μ^*	ΔE[b] /kJ mol^{-1}	
000	10.68	0.383	10.32	0.357	10.02	0.362	10.04	0.367	9.51	(0.01)
001	17.31	1.863	16.62	1.799	16.59	1.780	16.59	1.822	15.11	
010	12.43	1.537	11.90	1.494	11.48	1.470	11.49	1.501	11.03	(0.01)
011	19.33	2.910	18.41	2.825	18.21	2.793	18.22	2.778	16.78	
012	14.06	1.692	13.69	1.644	13.61	1.637	13.60	1.633	12.39	
100	10.81	2.091	10.27	2.027	10.16	2.003	10.16	1.980	9.78	(0.02)
101	17.97	2.475	17.08	2.392	17.23	2.369	17.23	2.368	15.82	
102	16.88	0.511	16.09	0.494	16.24	0.488	16.24	0.471	14.89	
110	13.49	2.933	12.84	2.849	12.53	2.814	12.53	2.789	12.46	
112	16.08	2.085	15.44	2.022	15.45	2.008	15.45	2.006	14.40	
120	0.0	2.424	0.0	2.376	0.0	2.354	0.0	2.325	0.0	(0.86)
122	7.34	2.472	6.95	2.419	7.23	2.395	7.23	2.362	5.72	(0.09)
Thermally averaged dipole moments/μ^*[c]		2.402		2.350		2.323		2.296	2.290[d]	

a) Conformation with respect to O1–C1, C1–C2, and C2–O2 bonds. 0 for *trans* (180°), 1 and 2 for *gauche* (±60°). b) Relative energy to the most stable conformer 120. The absolute energies are −269.6531529, −269.6598670, −269.6676805, −269.6677203, and −269.1119519 Hartrees at B3LYP/6-311+G(2d,p)//B3LYP/6-311+G(2d,p), B3LYP/6-311+G(3d,2p)//B3LYP/6-311+G(2d,p), B3LYP/6-311++G(3df,3pd)//B3LYP/6-311+G(2d,p), B3LYP/6-311++G(3df,3pd)//B3LYP/6-311++G(3df,3pd), and G2 methods, respectively. c) At 298 K using Boltzmann formula. d) B3LYP/6-311++G(3df,3pd)//B3LYP/6-311++G(3df,3pd) dipole moments are used.

Table 7. Calculated Relative Energies ΔE, Dipole Moments μ, and Thermally Averaged Dipole Moment of $C_2H_5OC_2H_4OH$, (C_2E_1) at the B3LYP Level:[a] Populations[e] of Conformers are in Parentheses; $\mu^* = 3.33564 \times 10^{-30}$ C m

Conformation[c]	6-311+G(2d,p)		6-311+G(3d,2p)[b]		6-311++G(3df,3pd)[b]		
	ΔE[d] /kJ mol^{-1}	μ/μ^*	ΔE[d] /kJ mol^{-1}	μ/μ^*	ΔE[d] /kJ mol^{-1}	μ/μ^*	
0000	10.73	0.492	10.36	0.464	10.05	0.463	
0100	12.44	1.455	11.92	1.418	11.49	1.395	
0120	14.16	1.579	13.68	1.537	13.70	1.530	
1000	10.72	2.117	10.17	2.058	10.07	2.035	(0.01)
1100	13.42	2.832	12.76	2.761	12.43	2.727	
1200	0.0	2.479	0.0	2.435	0.0	2.414	(0.78)
1201	5.50	2.573	5.28	2.528	5.56	2.513	(0.08)
1202	6.46	2.526	6.23	2.482	6.48	2.468	(0.06)
1220	7.17	2.544	6.74	2.494	7.12	2.473	(0.04)
1222	12.38	2.743	11.90	2.691	12.35	2.672	
Thermally averaged dipole moments/μ^*[e]							
		2.466		2.417		2.392	
		2.474[f]		2.427[f]		2.402[f]	

a) The lowest 10 of total 31 conformers are shown. b) Single point calculations at the B3LYP/6-311+G(2d,p) geometries. c) Conformation with respect to O1–C1, C1–C2, C2–O2, and O2–C3 bonds. 0 for *trans* (180°), 1 and 2 for *gauche* (±60°). d) Relative energy to the most stable conformer 1200. The absolute energies are −308.9837590, −308.9912517, and −309.0001171 Hartree at B3LYP/6-311+G(2d,p), B3LYP/6-311+G(3d,2p), and B3LYP/6-311+G(3df,3pd), respectively. e) At 298 K using Boltzmann formula. f) All conformers with the relative energy <15.0 kJ mol^{-1} are considered at Boltzmann formula.

quency shift by forming intermolecular hydrogen bonds in C_1E_1 dimers. Since a typical shift due to the formation of an intermolecular hydrogen bond amounted to 160 cm^{-1}, as will be mentioned later in details, the results strongly suggest that the intramolecular hydrogen bonds are rather weak.

Thermally averaged dipole moments using the Boltzmann distribution with suitable degeneracy factors are also contained in Table 6. The dipole moments based on 6-311+G(2d,p) showed a slightly large discrepancy to that of 6-311++G(3df,3pd), contrary to the discrepancy in energy; they were 2.40 and 2.30 D, respectively, and the difference amounted to 0.1 D. Inclusion of a set of d and p functions, viz. 6-311+(3d,2p), improved the difference to 2.35 D, which was only about 0.05 D larger than the result obtained by 6-311++G(3df,3dp). They are favorable when compared with the experimental value of 2.13 D, but the calculations gave a larger value by about 0.17 D. Similar discrepancies were also found in small alcoholic systems such as CH_3OH.[31] Apart from the small discrepancies, the present results are useful for a qualitative discussion as described below.

B3LYP calculations have been reported to overestimate the effect of hydrogen bonding.[38] Comparison of the present G2 calculation with that of B3LYP/6-311++G(3df,2pd) results shows that the G2 method gives smaller relative energies. The largest differences were found for the conformers 122 and 012, but they were within 1.5 kJ mol^{-1} and the discrepancies for other conformers were within 0.5 kJ mol^{-1}. Therefore, the present calculations are considered to be meaningful for the comparison with the experimental results.

A significant conflict is found between previous works and the present work. The MP2/6-31+G(d) and HF/4-21G calculations[21,23] showed overestimates by 3 to 10 kJ mol^{-1}, except for 120 and 122 conformers, in comparison with the G2 results. Other ab initio calculations also gave similar discrepancies.[12–15,20,24,25]

A total of 35 conformations are possible for the C_2E_1 system. Among them, 31 conformations gave minima at geometry optimizations. The relative energies of the lowest 10 are summarized in Table 7. The last of the four numbers in the leftmost column represents the rotation angle of O_2(ether)–C_3 ($C_2O_2C_3C_4$ dihedral angle) as shown in Fig. 6b. Thermally averaged dipole moments contained in the table were calculated by including the contributions of all the conformations.

The relative energies of the ten C_2E_1 conformers in Table 7 agreed with each other among the three basis sets within an allowance of 1 kJ mol^{-1} as in the case of C_1E_1. The conformer 1200 had the lowest energy, which was followed by 1201 and 1202. The differences in these structures are essentially related to the orientation of the terminal CH_3 group. The energy differences of 6 kJ mol^{-1} in favor of the *trans* conformation agreed with the *trans–gauche* energy differences of alkanes.[40] The conformers with indices 122, 1220 and 1222 had the next lowest energies. They were 6 to 7 kJ mol^{-1} higher than the 120 group. The values were compared with 7.2 kJ mol^{-1} at the C_1E_1, resulting from 6-311++G(3df,3pd), and were essentially the same. The order of the relative energies for other conformer groups was also the same as the C_1E_1 conformers. Previous work using the 3-21G(d) basis set[14] agrees with our result within a few kJ mol^{-1} for the lowest five conformers that are correlated to the lowest two conformers of C_1E_1. However, it is quite probable that, for the conformers with higher energy that are not calculated in the work, a large discrepancy may be found compared to our results as mentioned for C_1E_1.

The calculated dipole moments became smaller by using the larger basis sets. The value for C_2E_1 was 2.42 D with 6-311+G(3d,2p) and 2.39 D with 6-311++(3df,3pd). The best

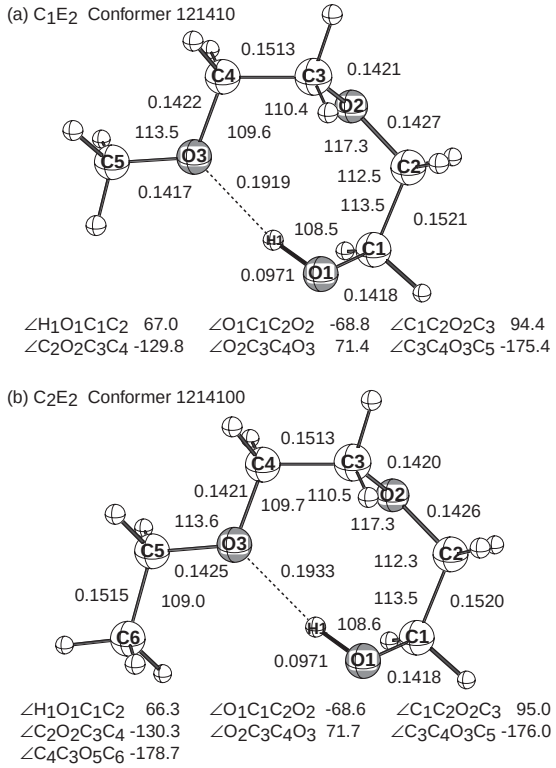

Fig. 7. Calculated geometries of C_1E_2 and C_2E_2 by the B3LYP/6-311+G(2d,p) method. Units are shown in nm and degree.

calculated moments, 2.39 D, should be compared with that of C_1E_1, 2.32 D. The experimental difference in the μ values between C_1E_1 and C_2E_1 was 0.05 D. Thus, a tendency of the dipole moment to increase the methyl group in the C_nE_1 system is well reproduced in the calculations, even though a small discrepancy of 0.2 D was found.

Calculated Dipole Moments of C_1E_2 and C_2E_2. On C_1E_2, six rotational angles are required to characterize their conformations. Their labels can be written as n_1n_2, where n_1 is a triplet of figures characterizing the first three rotational angles with respect to the O_1–C_1, C_1–C_2, and C_2–O_2 bonds, and n_2 is a triplet of other figures characterizing the last three rotational angles with respect to the O_2–C_3, C_3–C_4, and C_4–O_3 bonds. The numbering of the atoms is shown in Fig. 7a. There can be 364 conformers if *trans* and two *gauche* on each rotational angle are taken into consideration. Besides them, we found that on the rotation with respect to the O–C bonds, new minima emerged at about $\pm120^\circ$. This leads to the realization that there are more than a thousand conformers. In order to reduce the number of conformers and make calculations manageable, a threshold value was introduced for selecting representative conformations of C_1E_2. Contribution of conformers with a higher energy to the dipole moment can be negligible because the probability of such conformers should be small according to the Boltzmann distribution. Hence, if the energy of a conformer is greater than the threshold value, the conformations will be discarded from evaluations of thermally averaged dipole moments. We used 15 kJ mol^{-1} for the threshold value, which corresponds to a probability of 0.2% and an error in μ of about 0.01 D for C_2E_1, as shown in Table 2. Thus, our method of introducing the threshold value is quite acceptable.

The relative energies of the conformers can be estimated from the result of C_1E_1. It can be seen from Table 6 that the conformers of C_1E_1 could be classified into two groups, those above and below the threshold value. It was also observed that the conformations of C_1E_2 with $n_2 = 000$, 010, 020, 120, or 210 showed relatively lower energies, within a few kJ mol^{-1}, and the other ones had much higher energies. Those findings lead to a selection of conformations of C_1E_2 in the following way. Let n_a and n_b be the labels of C_1E_1 conformations with energies above and below the threshold, respectively. For n_1 equal to n_b, the geometries of the C_1E_2 conformers with all possible n_2, viz., 27 in total, were prepared. For conformers with $n_1 = n_a$, the five conformations for n_2 were taken into account. During the optimizations, new stable structures with the rotational angles $\pm120^\circ$ about the C–O bonds were obtained. All had intramolecular hydrogen bonds; therefore, in addition to the three angles of 180° and $\pm60^\circ$, we generated geometries of conformations with the rotational angles of $\pm120^\circ$ for the C–O bonds. Among them, the structures with a bond distance between H(alcohol) and O(ether) less than 0.3 nm were selected. About 300 conformations of C_1E_2 were the subjects of the calculations in which the B3LYP/6-311+G(2d,p)//B3LYP/6-31G(d)[39] method was employed. As a result, if the energies of conformers were smaller than 10 kJ mol^{-1}, the geometries of the conformers were optimized by B3LYP/6-311+(2d,p), and energies and dipole moments were obtained by B3LYP/6-311+(3d,2p) and 6-311++(3df,3pd). For the conformers with energies within 10 to 15 kJ mol^{-1}, the energies and dipole moments were recalculated using the 6-311+(3d,2p) basis set at the 6-31(d) geometries. Conformations with energies larger than 15.0 kJ mol^{-1} were discarded from the evaluations of thermally averaged dipole moments. We can safely obtain all conformations below the threshold energy by this systematic procedure. The results are summarized in Table 8.

Agreements of relative energies obtained by different basis sets are satisfactory and they are within 1 kJ mol^{-1} as have been shown in the C_nE_1 systems. The most stable conformer was 121410, where numbers 3 and 4 were used for $\pm120^\circ$ rotational angles, respectively. An intramolecular hydrogen bond is formed between H_1 and O_3 with the distance of 0.192 nm, as displayed in Fig. 7a, which cannot be observed in the C_1E_1 systems. This type of hydrogen bond is much stronger than that of C_1E_1 judging from the distances. The stability of the conformation, thus, is due to this strong intramolecular hydrogen bond. Conformers with $n_1 = 120$ give lower energies. It suggests that the relative energies of them are mainly determined by the first 3 angles, and then, small modifications to the energies are made by the last three angles, unless steric hindrances do not exist. This can be observed in most of the other conformers and it justifies the selection procedure used on the conformations mentioned before. Conformers 123220 and 122320 had intramolecular hydrogen bonds as in 121410 and were relatively lower energies due to the hydrogen bonds. They showed slightly longer distances (0.213 and 0.207 nm, respectively) than that of 121410.

For calculated dipole moments, small differences were

Table 8. Calculated Relative Energies ΔE, Dipole Moments μ, and Thermally Averaged Dipole Moment of $CH_3O(C_2H_4O)_2H$, (C_1E_2) at the B3LYP Level:[a] Populations[d] of Conformers are in Parentheses; $\mu^* = 3.33564 \times 10^{-30}$ C m

Conformation[c]	6-311+G(2d,p)		6-311+G(3d,2p)[b]		6-311++G(3df,3pd)[b]		
	ΔE[d] /kJ mol^{-1}	μ/μ^*	ΔE[d] /kJ mol^{-1}	μ/μ^*	ΔE[d] /kJ mol^{-1}	μ/μ^*	
121410	0.0	2.437	0.0	2.400	0.0	2.386	(0.21)
120000	1.31	1.922	1.58	1.883	1.43	1.874	(0.12)
120010[i]	0.69	3.271	0.89	3.205	0.63	3.172	(0.16)
120011	6.81	3.400	6.75	3.335	6.73	3.304	(0.01)
120012	6.62	2.168	6.56	2.135	6.55	2.122	(0.02)
120020	1.82	2.520	1.93	2.467	1.65	2.445	(0.11)
120021	5.02	1.096	5.14	1.088	5.19	1.076	(0.03)
120100	6.65	2.917	6.64	2.868	6.85	2.841	(0.01)
120120	2.53	3.467	2.69	3.408	2.88	3.383	(0.07)
120210	3.81	2.870	3.96	2.821	4.11	2.805	(0.04)
123220	3.98	2.587	3.88	2.543	4.48	2.527	(0.03)
122320	3.07	3.151	3.14	3.097	3.28	3.084	(0.06)
Threshold energy/kJ mol^{-1}		Thermally averaged dipole moments/μ^*[e]					
10.0		2.659[f]		2.612[f]		2.590[f]	
15.0		2.650[g]		2.600[h]		2.581[h]	

a) The lowest 12 (<7 kJ mol^{-1}) of total 62 conformers are shown. b) Single point calculations at the B3LYP/6-311+G(2d,p) geometries. c) Conformation with respect to O1–C1, C1–C2, C2–O2, O2–C3, C3–C4, and C4–O3 bonds. 0 for *trans* (180°), 1 and 2 for *gauche* (±60°), 3 and 4 for ±120° dihedral angles. d) Relative energy to the lowest conformer 120010. The absolute energies are −423.5344693, −423.5446276, and −423.5571109 Hartree at B3LYP/6-311+G(2d,p), B3LYP/6-311+G(3d,2p), and B3LYP/6-311++G(3df,3pd), respectively. e) At 298 K using Boltzmann formula. f) There are 23 conformers with the energies <10 kJ mol^{-1}. g) Additional 36 conformers with the energies 10 to 15 kJ mol^{-1} obtained at the B3LYP/6-311+G(2d,p)//B3LYP/6-31G(d). h) Additional 39 conformers with the energies 10 to 15 kJ mol^{-1} obtained at the B3LYP/6-311+G(3d,2p)//B3LYP/6-31G(d). i) The conformer seems to have very swallow potential surfaces for the rotations. The geometry was re-calculated using the B3LYP/6-311++(3df,3pd) with the gird = ultrafine and opt = tight options. The conformer was obtained at a minimum with the energy −423.5569363 Hartree.

found for the different basis sets employed here. Using the threshold energy of 15.0 kJ mol^{-1}, they were 2.65, 2.60, and 2.58 D, for 6-311+G(2d,p), 6-311+G(3d,2p), and 6-311++G-(3df,3pd), respectively. Reducing the threshold to 10 kJ mol^{-1} made no significant difference. For example, the value varied by only 0.01 D with 6-311++G(3df,3pd). From this fact, it is expected that contributions by higher energy conformers to the μ of C_1E_2 are small even though the density of conformers per unit energy becomes large. Our best value of μ was 2.581 D, which was calculated by the 6-311++G(3df,3pd) basis set with the 15 kJ mol^{-1} threshold energy and it is compared with the observed value of 2.476 D.

We found that an extension of the –(C_2H_4O)– group brought about a considerable change in μ. The value was increased by 0.26 D, which resulted from 6-311++G(3df,3pd)//6-311+G-(2d,p). It is slightly smaller than the experimental value by 0.35 D, and the deviation is acceptable. The increasing of μ is not explainable by a simple comparison between the μ of individual conformers of C_1E_1 and C_1E_2. The individual dipole moment of C_1E_2 conformers varied largely: for example, 2.39 D for 121410 and 1.43 D for 120000. Thus, the use of the Boltzmann formula for evaluating the dipole moments is quite important for molecules in which many isomers exist and their relative energies are close to each other.

The same procedure as mentioned for C_1E_2 was adopted for the C_2E_2 calculations. The B3LYP/6-311+G(3d,2p)//B3LYP/6-311+(2d,p) and B3LYP/6-311++G(3df,3pd)//B3LYP/6-311+(2d,p) methods were employed for the rotational isomers that have the same conformations except for the terminal methyl group in those of C_1E_2 with an energy smaller than 10 kJ mol^{-1}. If the corresponding energies for C_1E_2 were within 10 to 15 kJ mol^{-1}, the energies and dipole moments were recalculated using the 6-311+(3d,2p) basis set at the 6-31(d) geometries.

The calculations gave rise to the lowest conformer of 1214100 as shown in Table 9. The relative energies for 1200100, 1200000, 1200200, and 1201200 were 0.65, 1.38, 1.62, and 3.01 kJ mol^{-1} at 6-311++G(3df,3pd), respectively. They and other conformers, such as 1201000 and 1232200, had very similar relative energies to the corresponding conformers of C_1E_2. Furthermore, *trans–gauche* energy differences with respect to the terminal methyl group were within 5 to 7 kJ mol^{-1}. Those findings indicate that a conformation about the terminal methyl group of C_2E_2 does not lead to a significant change of electronic states in this system from the corresponding C_1E_2, and the energy differences caused by the introduction of a terminal methyl group are attributed to the steric hindrance of the *trans–gauche* form.

The best dipole moments were found at the 6-311++G-(3df,3pd) basis set using a threshold of 15 kJ mol^{-1}. The value

Table 9. Calculated Relative Energies ΔE, Dipole Moments μ, and Thermally Averaged Dipole Moments of $C_2H_5O(C_2H_4O)_2H$, (C_2E_2) at the B3LYP Level:[a] Populations[e] of Conformers are in Parentheses; $\mu^* = 3.33564 \times 10^{-30}$ C m

Conformation[c]	6-311+G(2d,p)		6-311+G(3d,2p)[b]		6-311++G(3df,3pd)[b]		
	ΔE[d] /kJ mol^{-1}	μ/μ^*	ΔE[d] /kJ mol^{-1}	μ/μ^*	ΔE[d] /kJ mol^{-1}	μ/μ^*	
1200000	1.29	2.048	1.57	2.005	1.38	1.997	(0.10)
1200100	0.76	3.168	0.94	3.109	0.65	3.078	(0.14)
1214100	0.0	2.321	0.0	2.288	0.0	2.275	(0.18)
1214101	5.95	2.504	5.71	2.468	5.95	2.465	(0.02)
1214102	5.09	2.520	4.86	2.484	5.08	2.478	(0.02)
1200110	6.80	3.336	6.69	3.278	6.76	3.249	(0.01)
1200120	6.46	2.135	6.34	2.104	6.38	2.091	(0.01)
1200200	1.82	2.527	1.93	2.477	1.62	2.457	(0.09)
1200210	4.99	1.117	5.03	1.102	5.18	1.091	(0.02)
1201000	6.56	2.999	6.54	2.952	6.74	2.928	(0.01)
1201200	2.72	3.501	2.85	3.445	3.01	3.422	(0.05)
1202100	3.88	2.850	4.02	2.804	4.12	2.790	(0.03)
1232200	3.83	2.467	3.67	2.431	4.25	2.417	(0.03)
1223200	3.20	3.035	3.22	2.985	3.32	2.973	(0.05)
1200102	6.95	3.260	6.86	3.191	6.84	3.167	(0.01)
Threshold energy/kJ mol^{-1}		Thermally averaged dipole moments/μ^*[e]					
10.0		2.629[f]		2.584[f]		2.566[f]	
15.0		2.620[g]		2.575[h]		2.567[h]	

a) The conformers with energies <7 kJ mol^{-1} of total 96 conformers are shown. b) Single point calculations at the B3LYP/6-311+G(2d,p) geometries. c) Conformation with respect to O1–C1, C1–C2, C2–O2, O2–C3, C3–C4, C4–O3, and C4–C5 bonds. 0 for *trans* (180°), 1 and 2 for *gauche* (±60°), 3 and 4 for ±120° dihedral angles. d) Relative energy to the lowest conformer 1214100. The absolute energies are −462.8650771, −462.8760214, and −462.8895472 Hartree at B3LYP/6-311+G(2d,p), B3LYP/6-311+G(3d,2p), and B3LYP/6-311++G(3df,3pd). e) At 298 K using Boltzmann formula. f) There are 35, 36, and 34 conformers with the energies <10 kJ mol^{-1} for 6-311+G(2d,p), 6-311+G(3d,2p), and 6-311++G(3df,3pd) calculations, respectively. g) Additional 56 conformers with the energies 10 to 15 kJ mol^{-1} obtained at B3LYP/6-311+G(2d,p)//B3LYP/6-31G(d). h) Additional 60 conformers with the energies 10 to 15 kJ mol^{-1} obtained at B3LYP/6-311+G(3d,2p)//B3LYP/6-31G(d).

of 2.57 D for C_2E_2 should be compared with the calculated value of 2.58 D for C_1E_2. Increasing the methylene group, the dipole moment reduced contrary to the C_nE_1 systems, and the difference of 0.014 D resulting from the calculations agree well with the experimental one of 0.02 D.

Calculations of Vibrational Frequency for C_1E_1 Dimers. The vibrational spectrum for C_nE_m systems have been studied by a number of authors experimentally and theoretically.[12–15,20–23] From those works and the present work as mentioned previously, it is well established that the sharp peeks appearing at around 3600 cm^{-1} for C_1E_1 are assigned to the O–H vibration of the monomers with different conformations. The broad band around 3505 cm^{-1} is probably ascribed to the intermolecular aggregation of C_1E_1.[12] In previous theoretical studies, the relative energies and vibrational frequencies of C_1E_1 dimers built from 120 and 122 conformers have been calculated using the HF/3-21G(d)//AM1 method.[22] Because of the limitations of the method, it was quite difficult to obtain a quantitative assessment of the observed broad band. Our main goal here is to provide the origin of the broad band by a reliable theoretical method.

The relative and binding energies of all the C_1E_1 dimers calculated here are shown in Table 10. The dimer of 120–120, which consists of two 120 conformers, has the lowest energy. In the structure, a hydroxy group of the 120 conformer acts as a hydrogen donor and accepter, and it forms hydrogen bonds with the oxygen of the ether group and hydrogen of the alcohol of the second conformer as shown in Fig. 8c. The dimer 120–210c (C_2), made from 120 and its enantiomer 210, is the second lowest in energy, where both oxygens of the ether contribute to the formation of hydrogen bonding as illustrated in Fig. 8f. Its energy is only 1.4 kJ mol^{-1} above the most stable dimer. Then, complexes 120–120c (Fig. 8d) and 120–210 (Fig. 8e) follow with relative energies of 2.3 and 2.4 kJ mol^{-1}, respectively. We obtained those four dimers made from 120 conformers, including its enantiomer 210. They were also reported in an earlier study.[22] However, our results for their order and magnitude of relative energies are very different from that work. Other complexes in Table 10 are high in energies. Among them, the complexes 000–000 and 000–000d, which structures are shown in Figs. 8a and 8b, respectively, have highest energies. This can be explained by the relative energy of each component. For example, twice of 6.95 kJ mol^{-1}, which is the relative energy of the 122 monomer, is approximately equal to the energy of the complex 122–122, 13.37 kJ mol^{-1}, and the energy of 8.0 kJ mol^{-1} for 120–000 is close to the 10.3 kJ mol^{-1} of the conformer 000. It strongly suggests that the energies of the dimers are determined by their components

Table 10. Calculated Relative Energies ΔE, Dissociation Energies D_e, OH Frequencies $\tilde{\nu}$, and IR Absorption Coefficient A of the C_1E_1 Dimer[a)]

Conformation[b)]	B3LYP/6-311+G(3d,2p)//B3LYP/6-311+G(2d,p)		B3LYP/6-311+G(2d,p)					
	ΔE[c)] /kJ mol^{-1}	D_e[d)] /kJ mol^{-1}	$\tilde{\nu}$/cm^{-1}		($\Delta\tilde{\nu}$/cm^{-1})[e)]	A/km mol^{-1}		
000–000	27.76	−20.50	3677	(−175)	534	3843	(−9)	53
000–000d	28.06	−20.19	3662	(−190)	670	3850	(−2)	45
100–120	15.52	−22.36	3662	(−167)	652	3792	(−13)	48
120–000	8.04	−29.90	3603		142	3647		979
120–100	8.20	−29.73	3611		122	3652		909
120–120	0.0	−27.62	3606	(−199)	138	3648	(−157)	843
120–120c	2.32	−25.30	3654	(−151)	3	3670	(−135)	1063
120–122	6.96	−27.61	3601		173	3643		789
120–122c	9.50	−25.08	3654		33	3666		954
120–200	9.10	−28.79	3622		121	3659		800
120–210	2.39	−25.23	3632	(−173)	121	3665	(−140)	732
120–210c	1.73	−25.88	3676	(−129)	0	3688	(−117)	939
122–122	13.37	−28.16	3585	(−206)	224	3642	(−149)	755
122–122c	15.58	−25.94	3644	(−147)	77	3653	(−138)	951

a) Frequency shifts $\Delta\tilde{\nu}$ by dimerization are shown in parenthesis. b) Conformations of two C_1E_1 monomers. Each monomer is separated by minus sign, −. c) Relative energies to the most stable dimers, 120–120. The total energy is −539.330253909 Hartree at B3LYP/6-311+G(3d,2p)//B3LYP/6-311+G(2d,p). d) Binding energies D_e of dimerization. Total energies of 000, 100, 120, and 122 are −269.6559373, −269.6559568, −269.6598670, and −269.6572189 Hartree, respectively at B3LYP/6-311+G(3d,2p)//B3LYP/6-311+G(2d,p). e) B3LYP/6-311+G(2d,p) frequencies of monomers for 000, 100, 120, and 122 are 3852, 3828, 3805, and 3791 cm^{-1}, respectively.

qualitatively and small modifications in the energies take place due to the interactions between the two monomers.

It has been reported that B3LYP calculations overestimate hydrogen-bonding energies.[38] To test this point, calculations for a water dimer were carried out by B3LYP/6-311+G(2d,p) and B3LYP/6-311++G(3dp,3pd) methods. They gave rise to the binding energies, D_e, 23 and 20 kJ mol^{-1}, respectively. Those values are in very good accord with the one for the most reliable calculated energy, 21.0 kJ mol^{-1}.[41] We therefore expect that the hydrogen-bonded systems treated here do not suffer from overestimation of the binding energy and our B3LYP calculations show reliable results.

The OH frequencies of those dimers are shown in Table 10. It is noteworthy that all frequencies of the dimers are shifted to lower energies as expected, since the formation of intermolecular hydrogen bonds weaken the OH bonds. If dimers were formed, we would expect that complexes 120–120, 120–210c, 120–120c, and 120–210 make predominant contributions to the observed OH peaks and other complexes including the component 120, such as 120–122 and 120–100, probably giving a slight contribution to them. All such dimers have two hydrogen bonds, and therefore, low energy shifts take place in two OH vibrations. Furthermore, vibrations at the higher frequency always have much larger intensities than those at the lower frequency, as shown in the table. Thus, it is expected that a predominant contribution to the observed IR spectrum comes from the vibrations of larger intensities of each dimer. The computed frequencies for dimers were 3648 (120–120), 3688 (120–210c), 3670 (120–120c), and 3665 (120–210) cm^{-1}. It is well known that computed frequency values contain systematic errors and are scaled to eliminate the errors. We used the factor 0.96 for the 6-311+G(2d,p) basis set, which was obtained by comparison of the calculated and experimen-

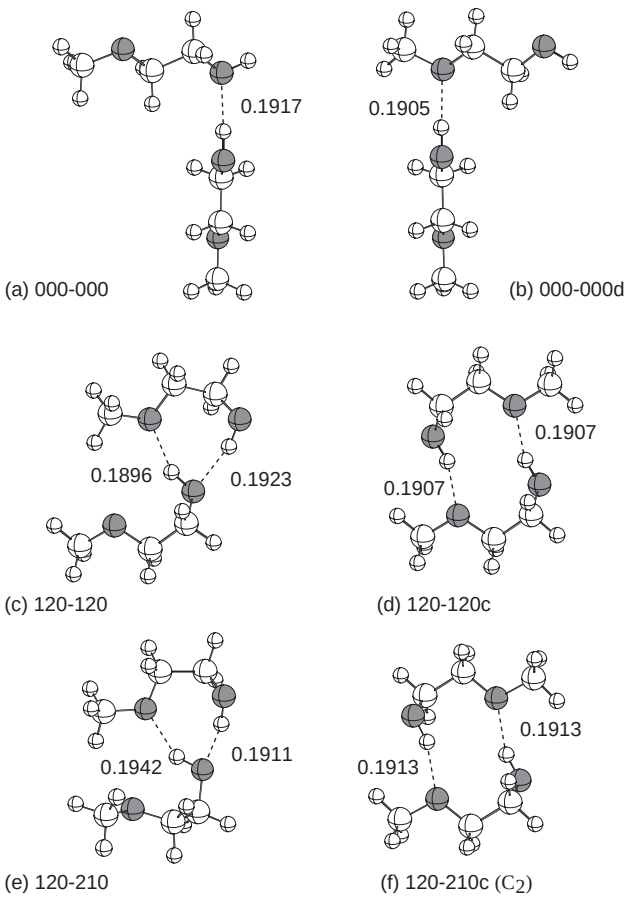

Fig. 8. Calculated geometries of C_1E_1 dimers by the B3LYP/6-31+G(2d,p) method. Hydrogen-bond lengths are shown in nm. Shadow circles picture O atoms.

tal OH frequencies of water and methanol. Applying the scale factor, they were reduced to 3502, 3540, 3523, and 3518 cm^{-1}, respectively. Those calculated values agree very well with the observed maximum. Therefore, we conclude that the broad band at 3505 cm^{-1} arises from the OH vibrations of the dimers made of the monomer 120 and the assignment proposed in previous works[8,10,11] should be completely ruled out.

References

1 K. Tsujii, *Surface Activity*, ed. by T. Tanaka, Academic Press, Tokyo, **1998**, Chap. 2.

2 R. Tanaka, *J. Colloid Interface Sci.* **1988**, *122*, 220.

3 R. Tanaka, A. Saito, *J. Colloid Interface Sci.* **1990**, *134*, 82.

4 R. Tanaka, M. Adachi, *Thermochim. Acta* **2003**, *404*, 133.

5 H. Matsuura, K. Fukuhara, *J. Phys. Chem.* **1987**, *91*, 6139.

6 H. Saito, T. Yonezawa, S. Matsuoka, K. Fukui, *Bull. Chem. Soc. Jpn.* **1966**, *39*, 989.

7 T. K. K. Srinivasan, C. I. Jose, A. B. Biswas, *Can. J. Chem.* **1969**, *47*, 3877.

8 M. Nakamura, T. Miura, N. Yano, Proceedings of the Seventh International Conference on Congr. Surf. Act. Subst., Moscow, **1976**, Vol. 2, p. 773.

9 L. S. Prabhumirashi, C. I. Jose, *J. Chem. Soc., Faraday Trans. 2* **1975**, *71*, 1545.

10 L. S. Prabhumirashi, C. I. Jose, *J. Chem. Soc., Faraday Trans. 2* **1976**, *72*, 1721.

11 L. S. Prabhumirashi, C. I. Jose, *J. Chem. Soc., Faraday Trans. 2* **1978**, *74*, 255.

12 F. P. S. C. Gil, R. Fausto, A. M. Amorim da Costa, J. J. C. Teixeira-Dias, *J. Chem. Soc., Faraday Trans.* **1994**, *90*, 689.

13 F. P. S. C. Gil, J. J. C. Teixeira-Dias, *THEOCHEM* **1995**, *332*, 269.

14 F. P. S. C. Gil, A. M. Amorim da Costa, J. J. C. Teixeira-Dias, *J. Phys. Chem.* **1995**, *99*, 8066.

15 M. H. Langoor, L. M. J. Kroon-Batenburg, J. H. van der Maas, *J. Chem. Soc., Faraday Trans.* **1997**, *93*, 4107.

16 R. L. Brinkley, R. B. Gupta, *Ind. Eng. Chem. Res.* **1998**, *37*, 4823.

17 F. A. J. Singelenberg, J. H. van der Maae, *J. Mol. Struct.* **1991**, *243*, 111.

18 F. A. J. Singelenberg, E. T. G. Lutz, J. H. van der Maae, *J. Mol. Struct.* **1991**, *245*, 173.

19 F. A. J. Singelenberg, J. H. van der Maae, L. M. J. Kroon-Batenburg, *J. Mol. Struct.* **1991**, *245*, 183.

20 H. Yoshida, K. Takikawa, K. Ohno, H. Matsuura, *J. Mol. Struct.* **1993**, *299*, 141.

21 S. Vazquez, R. A. Mosquera, M. A. Rios, C. V. Alsenoy, *J. Mol. Struct.* **1989**, *188*, 95.

22 F. P. S. C. Gil, A. M. Amorim da Costa, R. E. Roy, J. J. C. Teixeira-Dias, *J. Phys. Chem.* **1995**, *99*, 634.

23 M. Buck, *Phys. Chem. Chem. Phys.* **2003**, *5*, 18.

24 M. Takenaka, R. Tanaka, S. Murakami, *J. Chem. Thermodyn.* **1980**, *12*, 849.

25 R. H. Stokes, K. N. Marsh, *J. Chem. Thermodyn.* **1976**, *8*, 709.

26 R. Tanaka, H. Tsuzuki, K. Okazaki, T. Kinoshita, *Fluid Phase Equilib.* **1996**, *123*, 131.

27 R. Tanaka, T. Yokoyama, *J. Solution Chem.* **2004**, *33*, 1061.

28 H. Fröhlich, *Trans. Faraday Soc.* **1948**, *44*, 238.

29 J. G. Kirkwood, *J. Chem. Phys.* **1939**, *7*, 911.

30 L. Onsager, *J. Am. Chem. Soc.* **1936**, *48*, 1486.

31 M. El-Hefnawy, K. Sameshima, T. Matsushita, R. Tanaka, *J. Solution Chem.* **2005**, *34*, 43.

32 H. T. French, M. Koshla, K. N. Marsh, *J. Chem. Thermodyn.* **1988**, *20*, 1175.

33 a) C. Lee, W. Yang, R. G. Par, *Phys. Rev. B* **1988**, *37*, 758. b) B. Miehlich, A. Savin, H. Stoll, H. Preuss, *Chem. Phys. Lett.* **1989**, *157*, 200. c) A. D. Becke, *J. Chem. Phys.* **1993**, *98*, 5648.

34 a) A. D. McLean, G. S. Chandler, *J. Chem. Phys.* **1980**, *72*, 5639. b) R. Krishnan, J. S. Binkley, R. Seeger, J. A. Pople, *J. Chem. Phys.* **1980**, *72*, 650. c) T. Clark, J. Chandrasekhar, G. W. Spitznagel, P. V. R. Schleyer, *J. Comput. Chem.* **1983**, *4*, 294. d) M. J. Frisch, J. A. Pople, J. S. Binkly, *J. Chem. Phys.* **1984**, *80*, 3265.

35 L. A. Curtiss, K. Raghavachari, J. A. Pople, *J. Chem. Phys.* **1993**, *98*, 1293.

36 M. J. Frisch, G. W. Trucks, H. B. Schlegel, G. E. Scuseria, M. A. Robb, J. R. Cheeseman, V. G. Zakrzewski, J. A. Montgomery, Jr., R. E. Stratmann, J. C. Burant, S. Dapprich, J. M. Millam, A. D. Daniels, K. N. Kudin, M. C. Strain, O. Farkas, J. Tomasi, V. Barone, M. Cossi, R. Cammi, B. Mennucci, C. Pomelli, C. Adamo, S. Clifford, J. Ochterski, G. A. Petersson, P. Y. Ayala, Q. Cui, K. Morokuma, D. K. Malick, A. D. Rabuck, K. Raghavachari, J. B. Foresman, J. Cioslowski, J. V. Ortiz, A. G. Baboul, B. B. Stefanov, G. Liu, A. Liashenko, P. Piskorz, I. Komaromi, R. Gomperts, R. L. Martin, D. F. Fox, T. Keith, M. A. Al-Laham, C. Y. Peng, A. Nanayakkara, M. Challacombe, P. M. W. Gill, B. Johnson, W. Chen, M. W. Wong, J. L. Andres, C. Gonzalez, M. Head-Gordon, E. S. Replogle, J. A. Pople, *Gaussian 98, Revision A.7*, Gaussian, Inc., Pittsburgh, PA, **1998**.

37 M. El-Hefnawy, R. Tanaka, *J. Chem. Eng. Data* **2005**, *50*, 1651.

38 V. Barcone, C. Adamo, *J. Chem. Phys.* **1996**, *105*, 11007, and cited herein.

39 R. Ditchfield, W. J. Hehre, J. A. Pople, *J. Chem. Phys.* **1971**, *54*, 724.

40 J. McMurry, *Organic Chemistry*, John Wiley & Sons, Inc., **1999**.

41 W. Klopper, J. G. C. M. van Duijneveldt-van de Rijdt, F. B. van Duijneveldt, *Phys. Chem. Chem. Phys.* **2000**, *2*, 2227, and cited herein.

42 J. A. Riddick, W. B. Bunger, T. K. Sakano, A. Weissberger, *Organic Solvents: Physical Properties and Methods of Purification (Techniques of Chemistry)*, 4th ed., Wiley-Interscience, New York, **1986**, Vol. II.

43 A. J. Treszczanowicz, G. C. Benson, *J. Chem. Thermodyn.* **1977**, *9*, 1189.

44 R. Francesconi, C. Castellari, F. Comelli, *J. Chem. Eng. Data* **1999**, *44*, 1373.

45 G. C. Benson, C. J. Halpin, A. J. Treszczanowicz, *J. Chem. Thermodyn.* **1981**, *13*, 1175.

46 G. Douheret, A. Pal, *J. Chem. Eng. Data* **1988**, *33*, 40.

47 F. J. Carmona, J. A. Golzalez, I. G. La Fuente, J. C. Cobos, *J. Chem. Eng. Data* **1999**, *44*, 892.

48 A. Pal, S. Sharma, *J. Chem. Eng. Data* **1998**, *43*, 21.

49 J. Canosa, A. Rodriguez, J. Tojo, *Fluid Phase Equilib.* **1999**, *156*, 57.

50 L. Albuquerque, C. Ventura, R. Gonçalves, *J. Chem. Eng. Data* **1996**, *41*, 685.

51 T. Chiao, A. P. Thompson, *J. Chem. Eng. Data* **1961**, *6*, 192.